

A Short Overview on Low Mass Scalars at Future Lepton Colliders

Tania Robens ^{1,2} 
¹ Division of Theoretical Physics, Ruder Boskovic Institute, 10002 Zagreb, Croatia; trobens@irb.hr

² Theoretical Physics Department, CERN, 1211 Geneva 23, Switzerland

Abstract: In this manuscript, I give a short summary on scenarios with new physics scalars that could be investigated at future e^+e^- colliders. I concentrate on cases where at least one of the additional scalars has a mass below 125 GeV, and discuss both models where this could be realized, as well as studies which focus on such scenarios. This work is based on several overview talks I recently gave at the CEPC workshop, FCC week and ECFA future collider workshop, as well as a Snowmass White Paper.

Keywords: new physics models; collider phenomenology; extended scalar sectors



Citation: Robens, T. A Short Overview on Low Mass Scalars at Future Lepton Colliders. *Universe* **2022**, *8*, 286. <https://doi.org/10.3390/universe8050286>

Academic Editors: Giuseppe Latino, Lorenzo Viliani and Jinmin Yang

Received: 15 April 2022

Accepted: 16 May 2022

Published: 20 May 2022

Publisher's Note: MDPI stays neutral with regard to jurisdictional claims in published maps and institutional affiliations.



Copyright: © 2022 by the author. Licensee MDPI, Basel, Switzerland. This article is an open access article distributed under the terms and conditions of the Creative Commons Attribution (CC BY) license (<https://creativecommons.org/licenses/by/4.0/>).

1. Introduction

The discovery of a scalar which so far largely agrees with predictions for the Higgs boson of the Standard Model (SM) has by now been established by the LHC experiments (see e.g., [1,2]), with analyses of Run II LHC data further confirming this. In the European Strategy Report [3,4], a large focus was put on future e^+e^- colliders, especially so-called Higgs factories with center-of-mass (com) energies around 240–250 GeV. While these will on the one hand further help to determine properties of the scalar discovered at the LHC, and especially will help to determine in detail the parameters and shape of the scalar potential, it is also interesting to investigate their potential to search for additional scalar states. In general, such states can be realized by extending the scalar sector of the SM by additional gauge singlets, doublets, triplets, or other multiplets. Depending on the specific extension, these models then contain several additional neutral or (multiply) charged scalar states. Here, I concentrate on scenarios where at least one of these has a mass $\lesssim 125$ GeV.

In this work, I give a short overview on some models that allow for such light states, and point to phenomenological studies investigating such models. This should be viewed as an encouragement for further detailed studies in this direction. A preliminary version of this overview has been submitted as a Snowmass White Paper [5].

2. Models

2.1. Singlet Extensions

In singlet extensions (see e.g., [6–10]), the SM scalar potential is enhanced by additional scalar states that are singlets under the SM gauge group. In such scenarios, the coupling of the novel scalar(s) to SM particles is typically inherited via mixing, i.e., mass-eigenstates are related to gauge eigenstates via a unitary mixing matrix. The corresponding couplings and interactions are mediated via a simple mixing angle. In general, in such models, scalars have decay modes that connect them to both the SM as well as the novel scalar sector. If the additional states are singlets, all interactions to SM final states are rescaled by a mixing angle, such that:

$$g_{h_i, \text{SMSM}} = \sin \alpha_i \times g_{h_i, \text{SMSM}}^{\text{SM}}$$

for general SMSM final states, where h_i and α_i denote the respective scalar and mixing angle. Depending on the specific kinematics, also novel triple and quartic interactions are

possible, where the couplings depend on the specific values of the potential parameters. This allows in general for decays $h_i \rightarrow h_j h_k$. Naturally, one of the CP even neutral scalars of the model has to have properties that concur with current measurements by the LHC experiments.

In [11], the authors present the status of current searches for the process,

$$p p \rightarrow h_{125} \rightarrow h_i h_i \rightarrow X X Y Y, \quad (1)$$

which for such models can be read as a bound in

$$\sin^2 \alpha \times \text{BR}_{h_{125} \rightarrow h_i h_i \rightarrow X X Y Y}.$$

We display these results in Figure 1. Current bounds on the mixing angle for the 125 GeV-like state are around $|\sin \alpha| \lesssim 0.3$ [12], which in turn means that branching ratios $\text{BR}_{h_{125} \rightarrow h_i h_i \rightarrow X X Y Y}$ down to $\mathcal{O}(10^{-5})$ can be tested. In particular, the $\mu\mu\mu\mu$ final states in the low mass region give interesting constraints on the $h_{125} \rightarrow h_i h_i$ branching ratio down to ~ 0.03 .

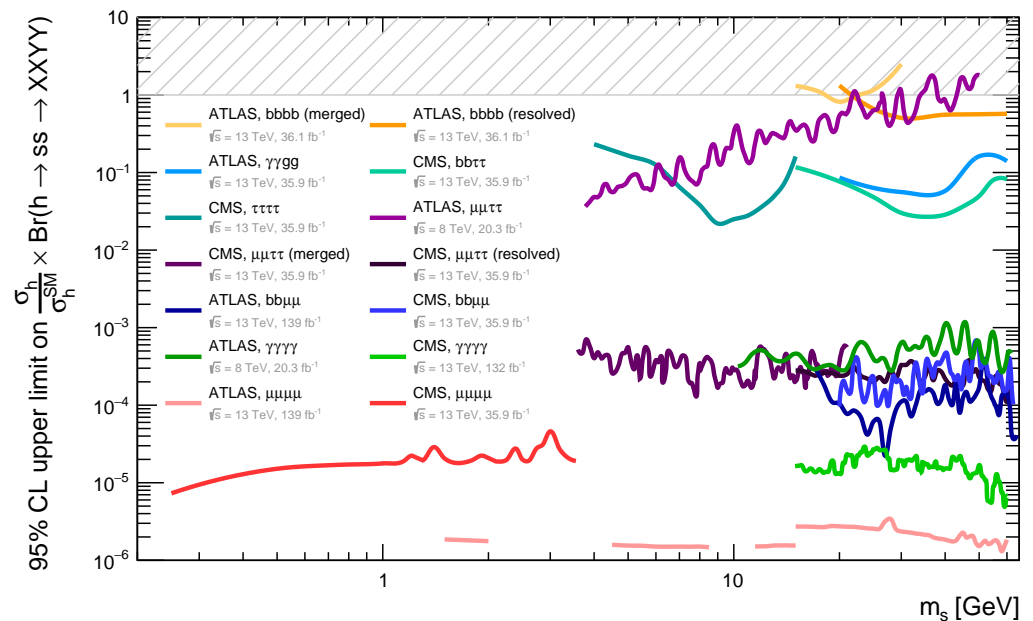


Figure 1. Limits on the process in Equation (1), taken from [11]. This displays current constraints which can especially be easily reinterpreted in extended scalar sector models, in particular models where couplings are inherited via a simple mixing angle. In this figure, the lighter scalar is denoted by s , which corresponds to h_i in the notation used in this manuscript.

We also refer the reader to a related discussion in [13].

After this short overview on current constraints, we now show an example of the allowed parameter space in a model with two additional singlets, the two real scalar extension studied in [10]. In this model, three CP-even neutral scalars exist that relate the gauge and mass eigenstates $h_{1,2,3}$ via mixing. One of these states has to have couplings and mass complying with current measurements of the SM-like scalar, the other two can have higher or lower masses. A detailed discussion of the model including theoretical and experimental constraints, can be found in [10]. In Figure 2, we display two cases where either one (high-low) or two (low-low) scalar masses are smaller than 125 GeV. On the y-axis, the respective mixing angle is shown. Complete decoupling would be designated by $\sin \alpha = 0$ in the notation used in this figure.

The points were generated using ScannerS [14,15], interfaced to HiggsBounds-5.10.2 [16–19] and HiggsSignals-2.6.2 [20,21], with constraints as implemented in these versions. Dominant decays are inherited from SM-like scalars with the respective masses, rendering the $b\bar{b}b\bar{b}$ final

state dominant for large regions of this parameter space. Note that in the case where both additional scalars have masses $\lesssim 125$ GeV, $h_1 h_1 h_1$ final states would also be allowed in certain regions of parameter space. Note that the points additionally fulfill the novel upper bound on the total width of the 125 GeV scalar of 5.6 MeV [22].

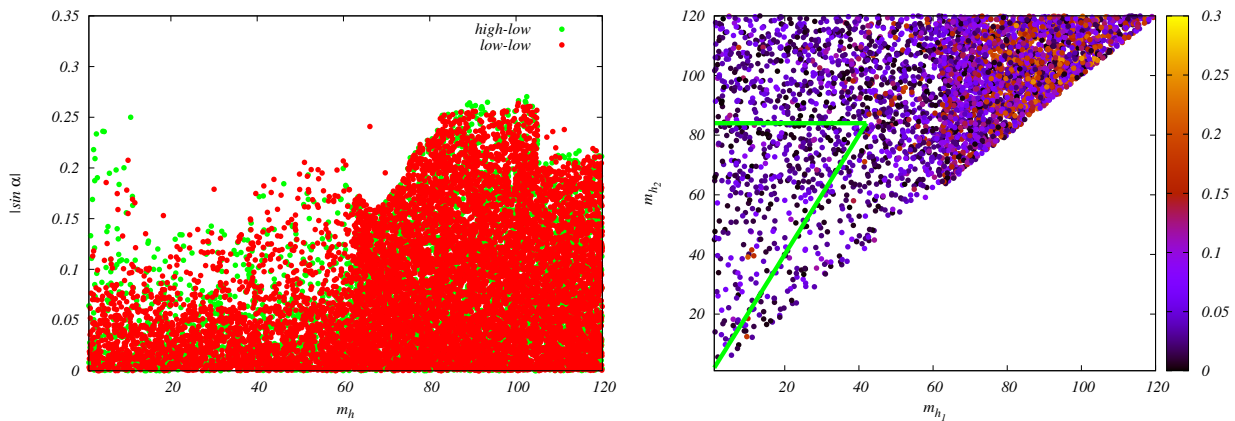


Figure 2. Available parameter space in the TRSM, with one (high-low) or two (low-low) masses lighter than 125 GeV. **Left:** light scalar mass and mixing angle, with $\sin \alpha = 0$ corresponding to complete decoupling. **Right:** available parameter space in the (m_{h_1}, m_{h_2}) plane, with color coding denoting the rescaling parameter $\sin \alpha$ for the lighter scalar h_1 . Within the green triangle, $h_{125} \rightarrow h_2 h_1 \rightarrow h_1 h_1 h_1$ decays are kinematically allowed.

2.2. Two Higgs Doublet Models

Two Higgs doublet models (2HDMs) constitute another example of new physics models allowing for low mass scalar states. A general discussion of such models is, e.g., given in [23] and will not be repeated here. In general, such models contain, besides the SM candidate, two additional neutral scalars which differ in CP properties as well as a charged scalar, so the particle content is given by h, H, A, H^\pm , where one of the two CP-even neutral scalars h, H needs to be identified with the 125 GeV resonance discovered at the LHC. Couplings to the fermions in the Yukawa sector distinguish different types of 2HDMs.

In [24], the authors perform a scan including bounds from theory, experimental searches and constraints, as e.g., electroweak observables, as well as B-physics. Examples for these scan results are shown in Figure 3, taken from that reference.

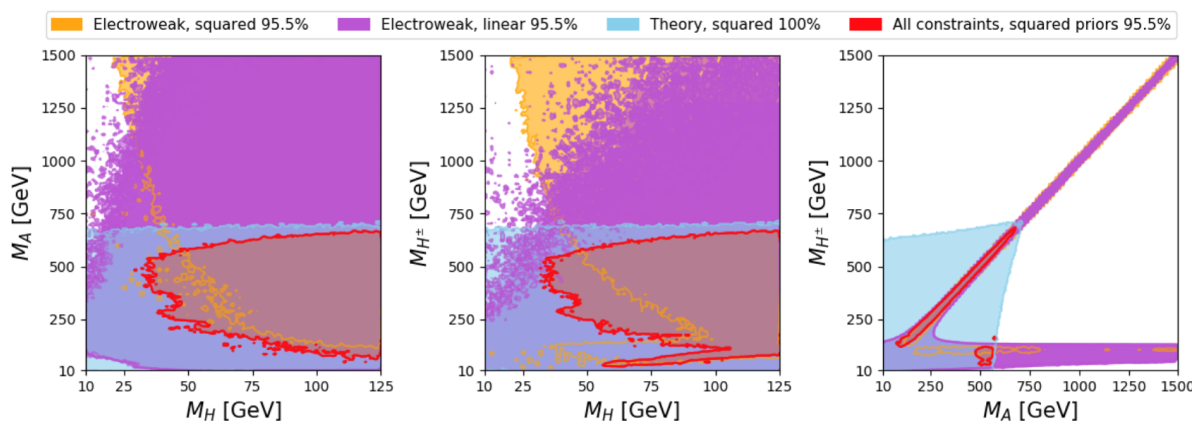


Figure 3. Allowed regions in the 2HDM, from a scan presented in [24].

We see that for all regions solutions for either one or several low mass scenarios exist and are viable for the constraints discussed in that reference. The authors here primarily

consider an aligned 2HDM [25,26], including an angle $\tilde{\alpha}$ that parametrizes the rescaling with respect to the Standard Model couplings to gauge bosons, with $\cos \tilde{\alpha} = 0$ designating the SM decoupling.

The limits on the absolute value of the cosine of rescaling angle vary between 0.05 and 0.25 [27]. In Figure 4, we display this angle vs the different scalar masses, reproduced from [24]¹. We see that all regions for masses $\lesssim 125$ GeV can be populated, with absolute value of mixing angle ranges $|\cos(\tilde{\alpha})| \lesssim 0.1$.

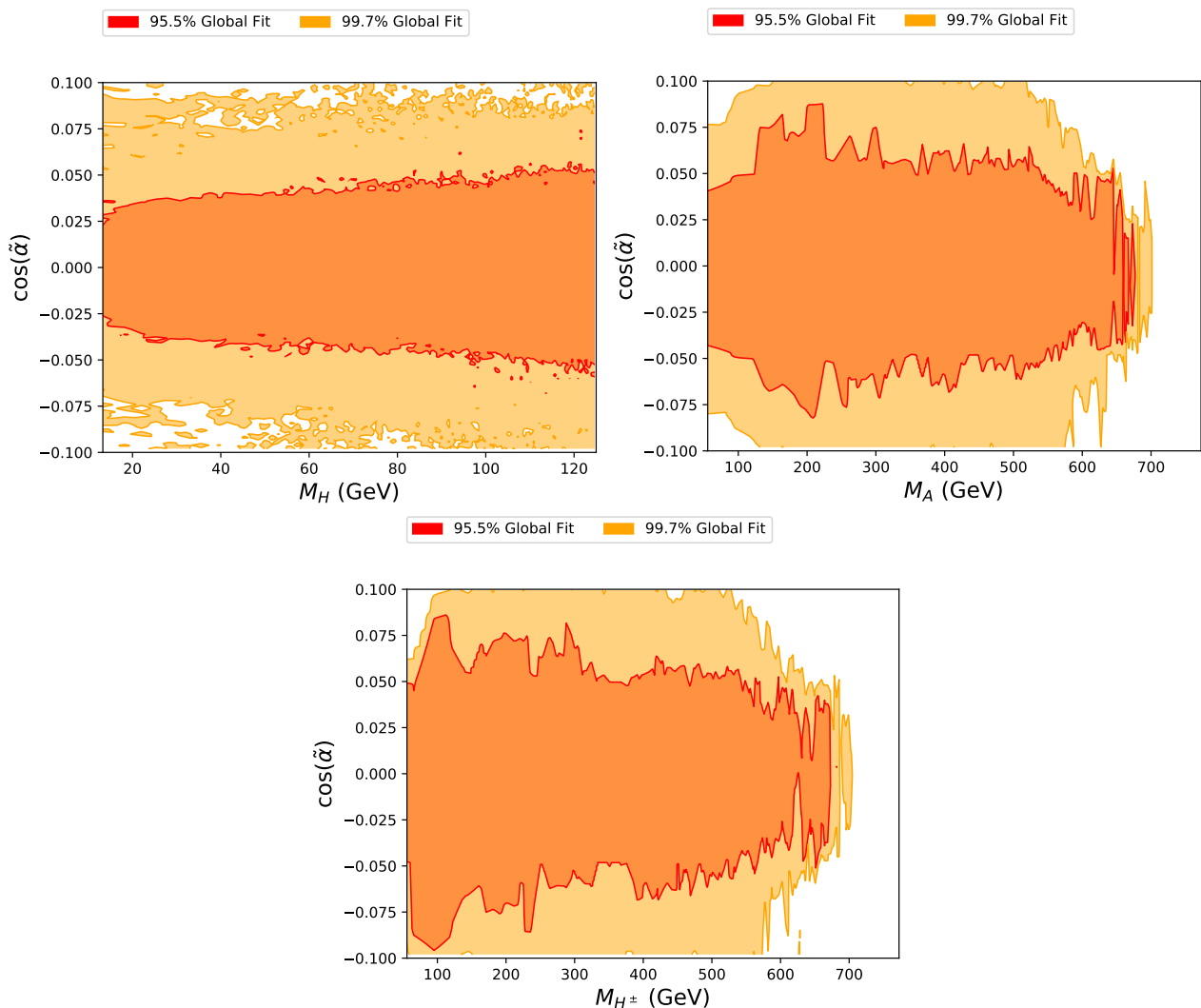


Figure 4. Mixing angle and masses of different additional scalars in the aligned 2HDM, from the scan presented in [24]. For all additional scalars, regions exist where masses are $\lesssim 125$ GeV, with absolute values of mixing angles such that $|\cos(\tilde{\alpha})| \lesssim 0.1$.

Other examples for 2HDMs including possibilities for low-mass scalars, in particular for the CP-odd candidate A , can be found in [28].

2.3. Other Extensions

The scalar sector of the SM can be extended by an arbitrary number of additional scalar fields, such as singlets, doublets, etc. One option which is also often considered is the extension of this sector by both singlets and doublets. We will discuss a couple of examples of such extensions which are able to provide regions where some of the additional scalars are in the low-mass range of interest here. For more details on the specific models, we refer the readers to the respective publications.

2.3.1. N2HDM

In [29], the authors consider a model where the SM scalar sector is extended by an additional doublet as well as a real singlet. This model has three CP even neutral scalar particles, out of which one needs to have the properties in compliance with LHC measurements of the 125 GeV scalar. The authors perform an extensive scan and find regions in parameter space where either one or both of the additional scalars have masses below 125 GeV. We show an example of the allowed parameter space in Figure 5. We see that in the CP-even sector there are regions within this model that still allow for low mass scalars.

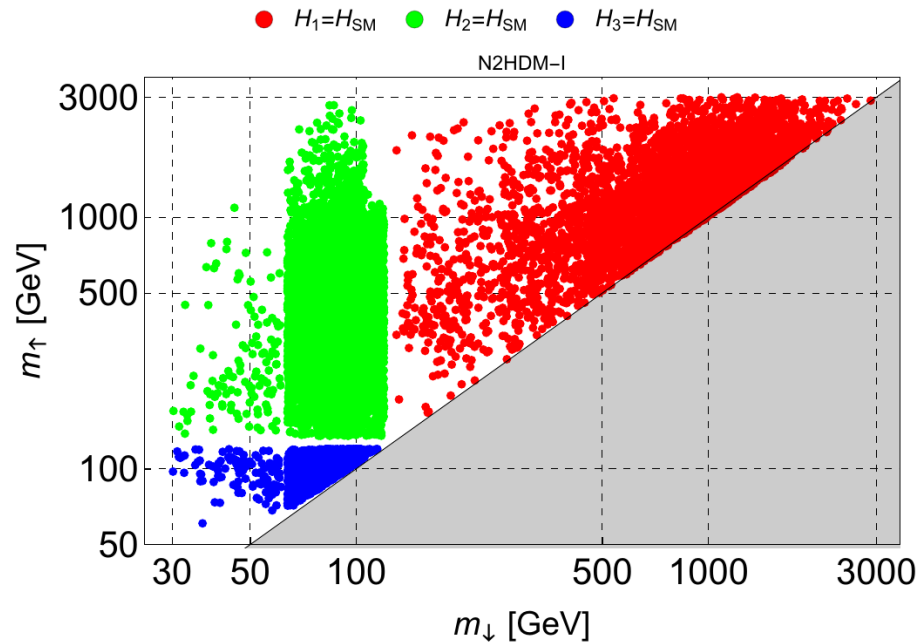


Figure 5. Scan results in the N2HDM, taken from [29]. There are regions in the models parameter space where either one or two of the additional scalars have masses $\lesssim 125$ GeV.

2.3.2. Lepton-Specific Inert Doublet Model

In [30], the authors consider a model where the SM scalar sector is augmented by an additional doublet, where they impose an exact \mathbb{Z}_2 symmetry. This symmetry is then broken by a specific coupling to the fermionic sector. The authors identify regions in the models parameter space that agree with current searches as well as anomalous magnetic momenta of electron and muon, and find regions where the second CP-even scalar can have a mass $\lesssim 30$ GeV. We display these regions in Figure 6.

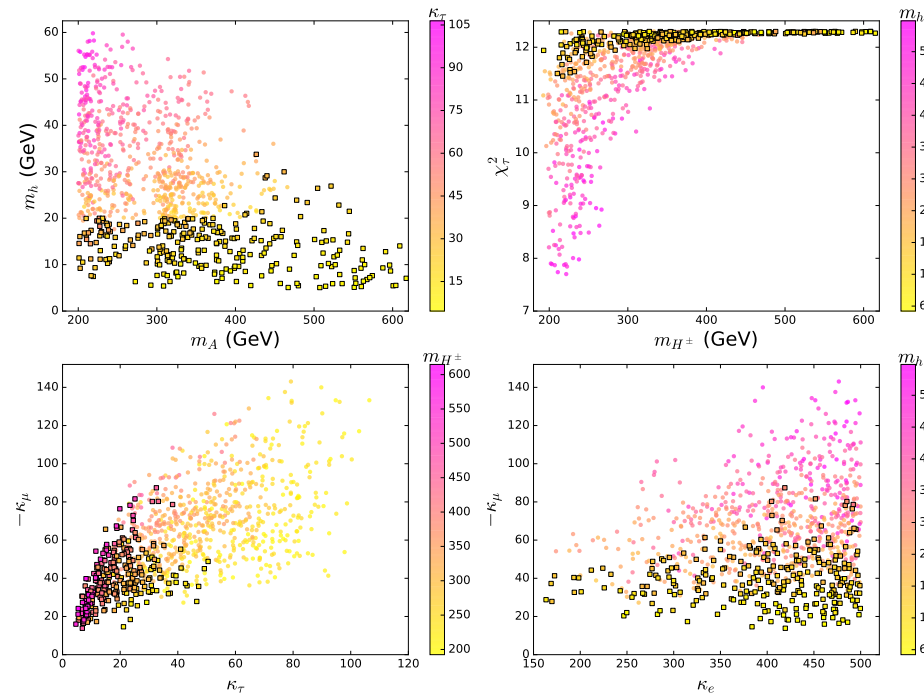


Figure 6. Allowed regions in the parameter space of the model discussed in [30], taken from that reference, where squares denote allowed and bullets excluded regions in the models parameter space. CP-even neutral scalars with low masses are viable within this model.

2.3.3. Scalar Triplet Model

Finally, we want to discuss a model containing scalar triplets, leading to a rich particle content as well as the possibility of CP violating terms. The model has been presented in [31]. This model contains 5 neutral, 3 charged, and 2 doubly charged mass eigenstates. The authors present regions in parameter space where masses for some of these can be $\lesssim 125$ GeV. We display these results in Figure 7. We see that both neutral and charged scalars with low mass realizations exist, with a rescaling of the hZZ coupling below LEP sensitivity. These scenarios could be investigated at future machines with higher sensitivity in this region.

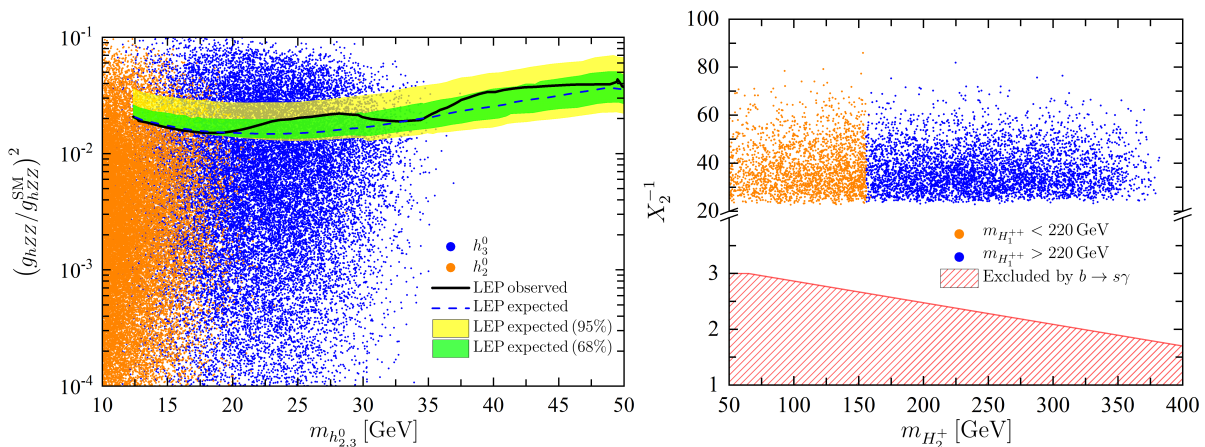


Figure 7. Allowed regions in the parameter space of the model discussed in [31], taken from that reference. For neutral and charged new scalars, masses $\lesssim 125$ GeV are achievable.

3. Studies at 90 GeV

For this center-of-mass energy, several searches exist which have already been performed at LEP and are summarized in [32,33], concentrating on Zh , $h_1 h_2$, and $h_1 h_1 h_1$ final states, where h_i signifies novel scalars. Possible new studies could build upon these searches. We want to note that the luminosity at FCC-ee and CEPC at this center of mass energy is exceeding LEP luminosity by several orders of magnitude [34,35].

We also want to draw attention to one specific study, which investigates several composite models at a com energy of 91 GeV [36]. The authors consider the process $e^+e^- \rightarrow \ell^+\ell^-\tau^+\tau^-$, where the tau-pair stems from an additional pseudoscalar a radiated off one of the fermion lines in the $\ell\ell$ pair-production. They apply a cut-based study as well as an improved analysis using machine learning techniques; for the latter, the authors are able to achieve a 3σ exclusion for benchmarks with masses $M_a \sim 20$ GeV. We display event rates for the various benchmark scenarios in Figure 8.

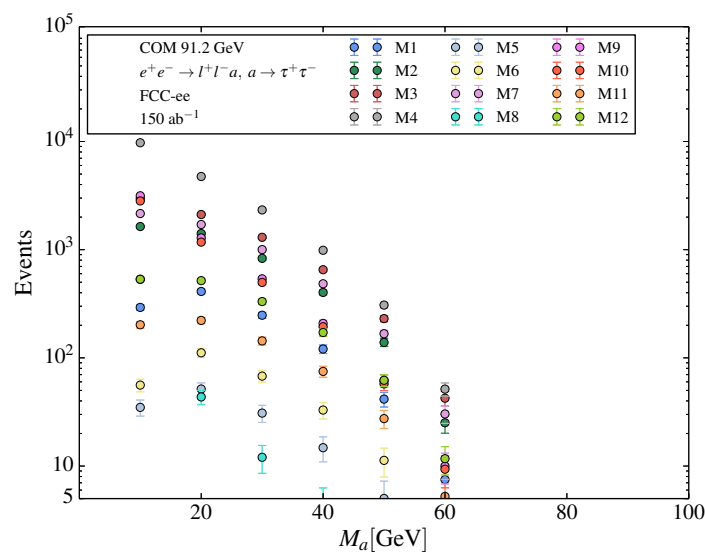


Figure 8. Rates at a 91 GeV FCC-ee for various models discussed in [36], for $\ell^+\ell^-\tau^+\tau^-$ final states. M7 and M10 reach a 3σ significance using ML techniques. Figure taken from [36].

4. Studies at 240–250 GeV

Throughout this work, we show for reference leading order predictions for Zh production at e^+e^- colliders for low mass scalars which are SM-like. These results were obtained using Madgraph5 [37] and are given for approximate reference only. We also display the VBF-type production of $e^+e^- \rightarrow h\nu_\ell\bar{\nu}_\ell$. Note that the latter signature also contains contributions from Zh production, where $Z \rightarrow \nu_\ell\bar{\nu}_\ell$.

Figure 9 shows the production cross sections for these processes for a center-of-mass energy of ~ 240 – 250 GeV. Using these predictions, and taking into account standard rescaling ~ 0.1 , around 10^5 – 10^6 events could be produced with ILC, FCC-ee, and CEPC design luminosities [34,35,38].

4.1. Dedicated Studies

4.1.1. Light Scalars in Zh Production

Not many dedicated studies exist that investigate low-mass scalars at Higgs factories. We here point to [39] that investigates the sensitivity of the ILC for low-mass scalars in Zh production, either using pure Z recoil (“recoil method”) or taking the light scalar decay into $b\bar{b}$ into account. The y-axis shows the 95 % CL limit for agreement with a background only hypothesis, which can directly be translated into an upper bound on rescaling. The authors validate their method by reproducing LEP results [33,40] for these channels prior to applying their method to the ILC. Their predictions are shown in Figure 10.

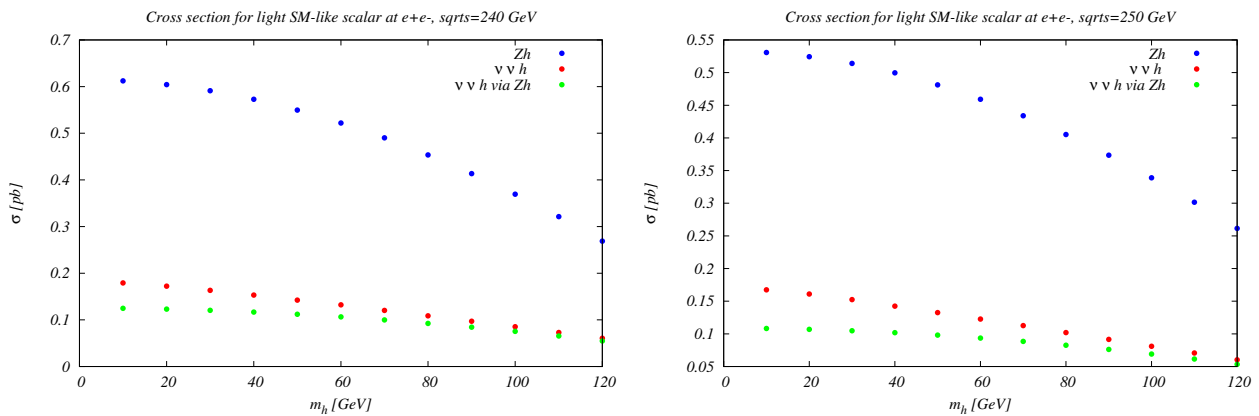


Figure 9. Leading order production cross sections for $Z h$ and $h \nu_{\ell} \bar{\nu}_{\ell}$ production at an $e^+ e^-$ collider with a com energy of 240 GeV(left) and 250 GeV (right) using Madgraph5 for an SM-like scalar h . Shown is also the contribution of $Z h$ to $\nu_{\ell} \bar{\nu}_{\ell} h$ using a factorized approach for the Z decay.

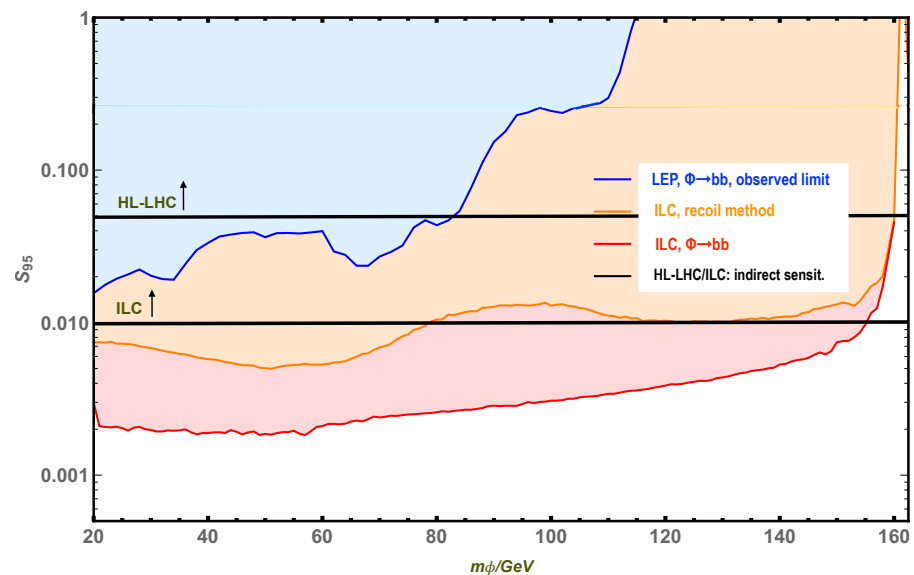


Figure 10. Sensitivity predictions for an ILC with a com energy of 250 GeV from [39]. See text for details.

A more detailed study along similar lines using the recoil method only and comparing different detector options has been presented recently in [41]. We display their results in Figure 11. The authors perform their analysis in a model where the coupling of the new resonance is rescaled by a mixing angle $\sin \theta$; therefore, their results can directly be compared with the ones presented in [39] and Figure 10.

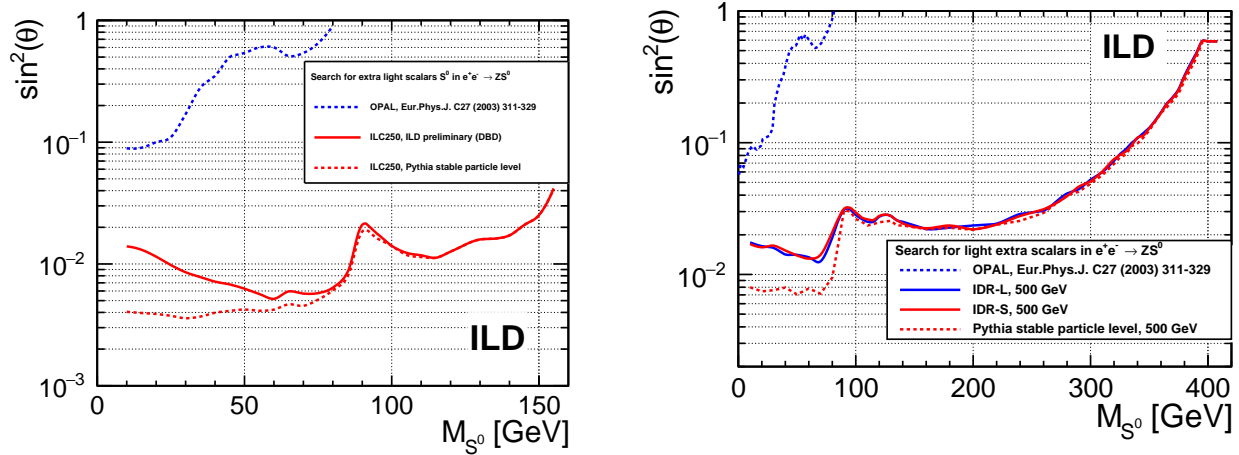


Figure 11. Upper bounds on the mixing angle for the model discussed in [41], in a comparison of different detector concepts and using the recoil method.

4.1.2. Higgsstrahlung and Decay into Two Light Scalars

In [42], the authors consider Higgs–Strahlung at a 240 GeV e^+e^- collider, where the Higgs subsequently decays into two light scalar states. They give 95 % confidence level bounds for the branching ratios into the decay products of the two light scalars as a function of the light scalar masses for an integrated luminosity of $\int \mathcal{L} = 5 \text{ ab}^{-1}$ following a detailed study. Their results are subsequently used by many authors as standard reference. We show their results for various channels in Figure 12.

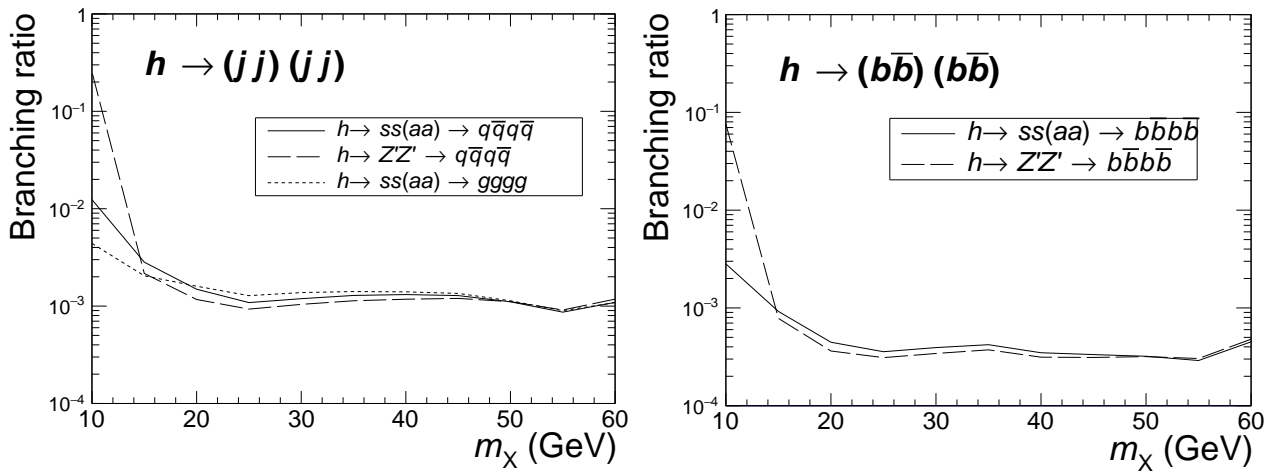


Figure 12. Ninety-five percent confidence bounds on branching ratios for Higgs decay into a pair of lighter particles, for a com energy of 240 GeV and $\int \mathcal{L} = 5 \text{ ab}^{-1}$. Taken from [42].

Depending on the mass, model, and decay mode, branching ratios down to $\sim 10^{-4}$ can be tested.

A more recent study [43] investigates the same process, but for 4 τ final states, for the same center-of-mass energy and integrated luminosity. The results, for varying values of tracking efficiency, are shown in Figure 13. Note that current constraints on the invisible branching ratio of the Higgs, the signal strength, as well as SM-like decays of the light scalars currently render a bound $\lesssim 10^{-2}$.

Several works make use of the bounds derived in [42]. In [44], the authors investigate the allowed parameter space in the scNMSSM, an NMSSM extension that relaxes unification requirements at the GUT scale [45–48], also known as NUHM, which contains in total five scalar particles; if CP is conserved, three are CP-even and two CP-odd. The authors include

various bounds on the models parameter space, and show the allowed scan points and predictions for the above channels for various scalar combinations. We display their results in Figure 14. We see that various scenarios exist where light scalars can be realized, with masses in the whole mass range between 10 and 60 GeV. The authors also display the projected sensitivity limits.

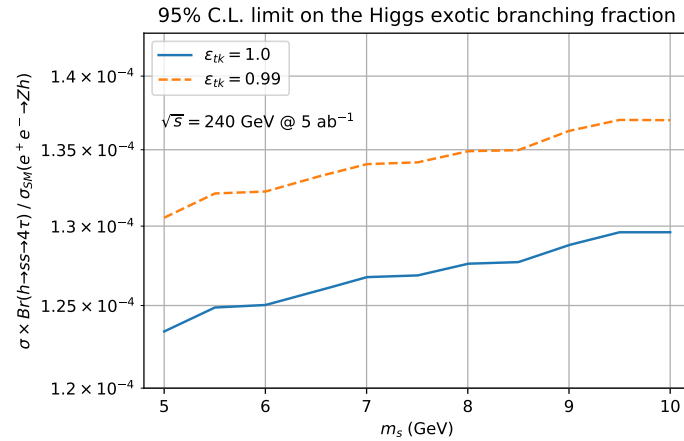


Figure 13. Bounds on decay of the SM Higgs boson into two light scalars, with a 4 τ final state, at an e^+e^- collider with a com energy of 240 GeV, with different assumptions on tracking efficiencies. Taken from [43].

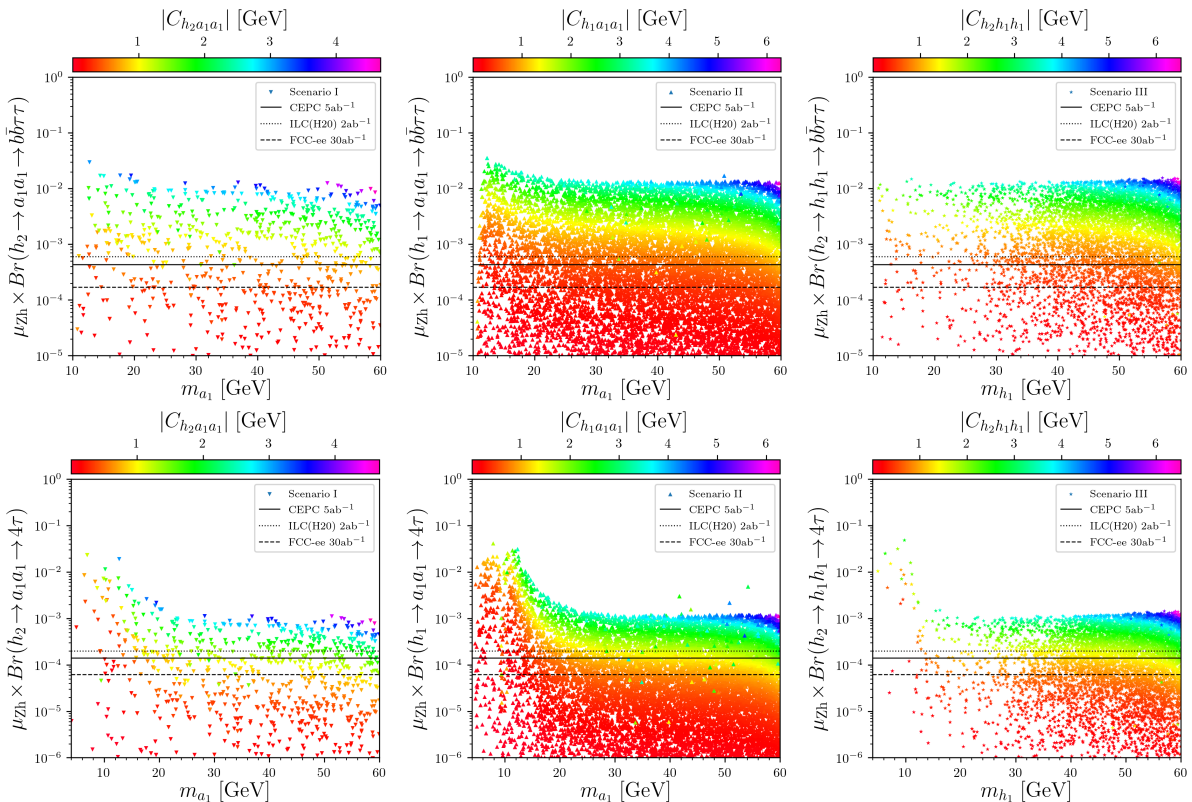


Figure 14. Allowed rates for various Higgs–Strahlung processes with successive decays into two light scalars. **Top:** $2b2\tau$ final state. **Bottom:** 4τ final state. Expected upper bounds for various collider machines are also shown, with projections from [42]. Figure taken from [44].

Finally, in simple singlet extensions it is possible to test regions in the models parameter space which can lead to a strong first-order electroweak phase transition. Several

authors have worked on this; we here show results from [49], where in addition several collider sensitivity projections are shown, including the bounds derived in [42]. From Figure 15, it becomes obvious that e^+e^- Higgs factories would be an ideal environment to confirm or rule out such scenarios. While [49] rely on previous analyses of this channel, in [50] the authors perform a dedicated study of this channel testing the same model and parameter space in the CEPC setup. Their results, also displayed in Figure 15, seem to confirm previous findings.

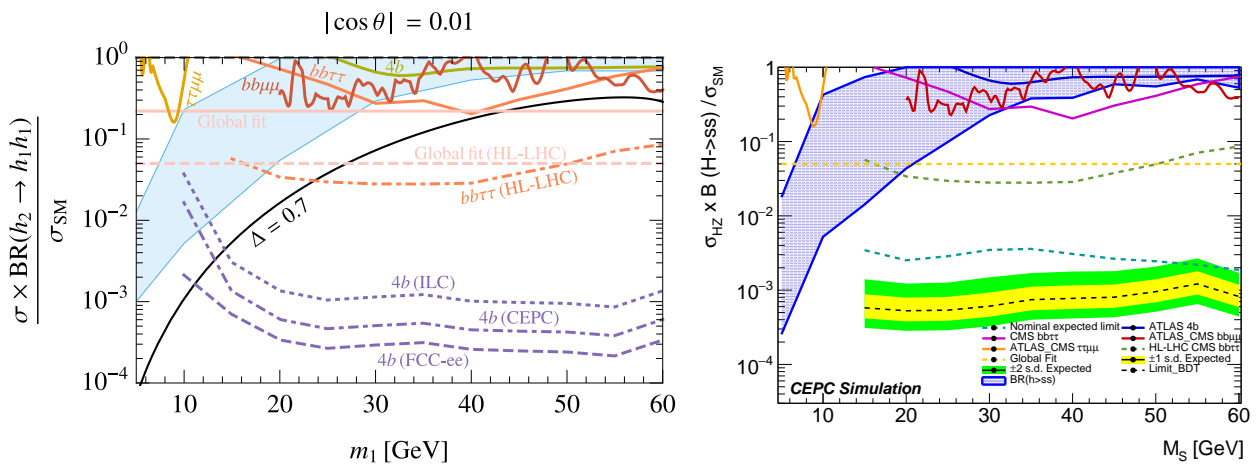


Figure 15. Expected bounds on Higgs production via Higgs–Strahlung and subsequent decay into two light scalars, in the singlet extension scenario discussed in [49,50]. **Left:** Taken from [49]. **Right:** Results presented in [50], for CEPC at 250 GeV. The blue band denotes the region where a strong first-order electroweak phase transition is possible. We see that e^+e^- Higgs factories are required on order to confirm or exclude such scenarios. LHC searches as well as projections stem from [51,52] ($bb\mu\mu$), [53] ($bb\tau\tau$), [54] ($4b$), and [55,56] ($\mu\mu\tau\tau$).

Related work, with a spontaneous breaking of the imposed \mathbb{Z}_2 symmetry, has been presented in [57].

4.1.3. Other Channels

We now turn to other channels that do not focus on Zh production and successive decays involving light scalars. We briefly present two different studies for such searches. In [58], the authors investigate a slightly different channel, i.e., tau pair-production where a light pseudoscalar is radiated off one of the outgoing fermion lines and decays again into $\tau^+\tau^-$, leading to a 4τ final state. They are considering a type X 2HDM, which in addition allows them to explain the current discrepancy between theoretical prediction and experiment for the anomalous magnetic momentum of the muon [59]. They perform a detailed study including background and determine 2 and 5 σ contours in the $(m_A, \tan\beta)$ plane, where $\tan\beta$ denotes the ratio of the vevs of the two doublets. Their results are shown in Figure 16. We see that even for 500 fb^{-1} , the proposed analysis can already test the region of interest to explain the $g_\mu - 2$ anomaly, including a possible discovery in that region of parameter space for 2 ab^{-1} .

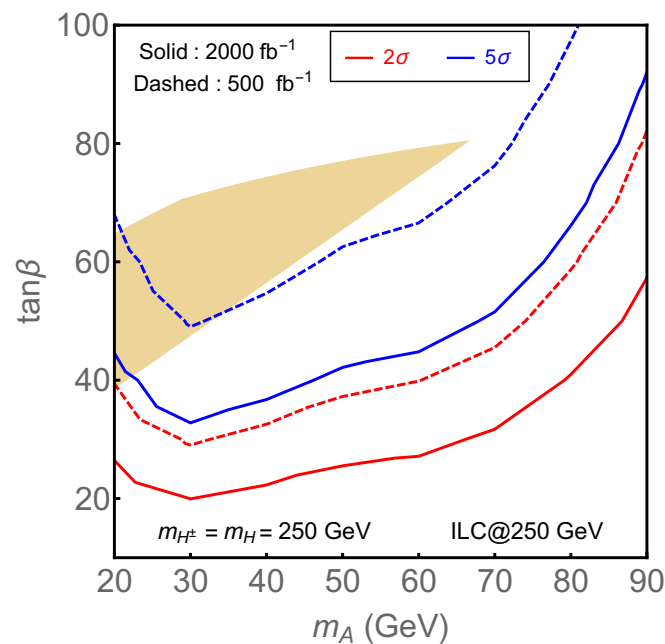


Figure 16. Exclusion and discovery regions in the 2HDM type X model, in the $(m_A, \tan \beta)$ plane. The color region additionally explains the current $g_\mu - 2$ discrepancy. Regions above the respective lines are excluded. Taken from [58].

It is also interesting to investigate models with give the possibility of light charged scalars. A corresponding study has been performed in [60], where the authors consider charged scalar pair-production within a 3HDM, with successive decays into $c\bar{c}b\bar{b}$ final states. The authors perform a detailed study and present their results in the 1 and 2 b-jet tagged category, as a function of light scalar mass and charm tagging efficiency. We show the corresponding significances in Figure 17, for a com energy of 240 GeV and an integrated luminosity of 1 ab^{-1} . Depending on the charm tagging efficiency, the authors predict that relatively large significances can be reached throughout the models parameter space.

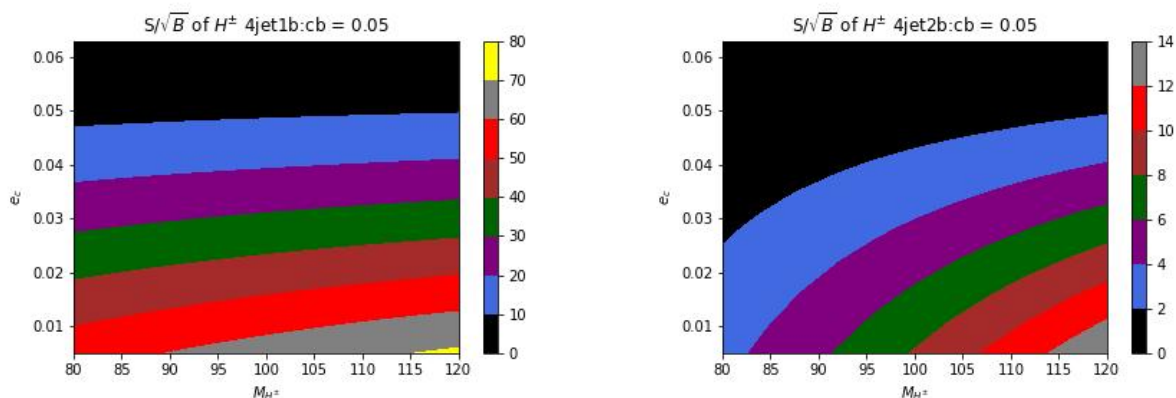


Figure 17. Significances as a function of charged scalar mass and charm tagging efficiency at an 240 GeV CEPC, at an integrated luminosity of 1 ab^{-1} , within a 3HDM as presented in [60], considering a $c\bar{c}b\bar{b}$ final state. Figures taken from that reference.

4.2. Cross Section Predictions

Inspired by possible low-mass excesses in LEP [33] and CMS [61], in [62] several models are fitted to these excesses that contain singlet and doublet extensions of the SM scalar sector; in particular, they consider models with an additional doublet as well as a

(complex) singlet, labelled N2HDM and 2HDMs, respectively. For both models, as well as varying $\tan\beta$ ranges (where $\tan\beta$ denotes the ratio of the vevs in the 2HDM part of the models), the authors investigate the possibility to explain the observed accesses and give rate predictions for a 250 GeV collider with a total luminosity of $\mathcal{L} = 2 \text{ ab}^{-1}$. We display their results in Figure 18. We see that also other final states for the h decay, as e.g., $\tau^+\tau^-$, gg , or W^+W^- can render sizeable rates. Related work concentrating on the N2HDM can be found in [63].

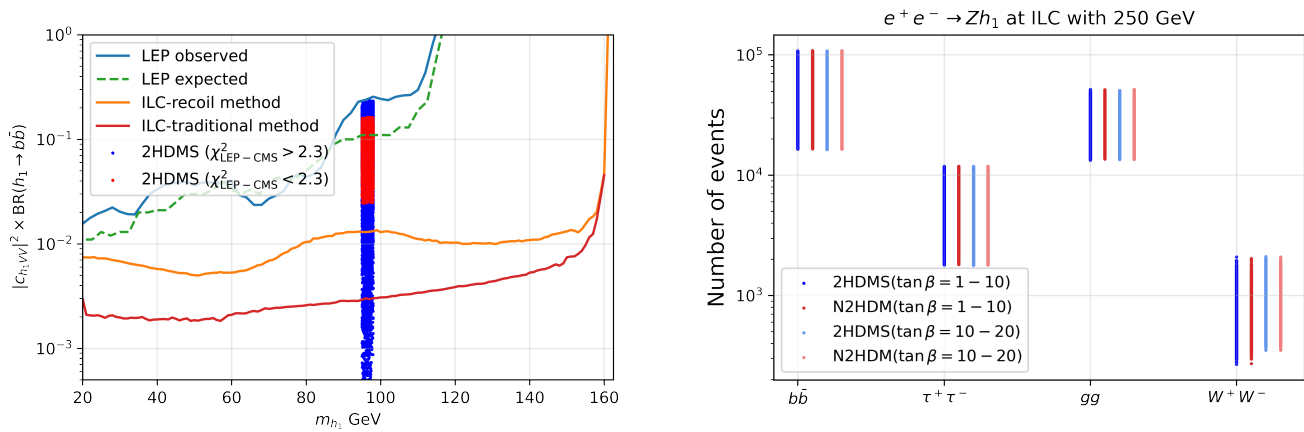


Figure 18. Left: Points in the 2HDMs that agree with both CMS and LEP excess and which can be probed at the ILC. Right: predicted rates in the 2HDMs and N2HDM at 250 GeV using full target luminosity.

5. Other Center of Mass Energies

The FCC-ee and CEPC colliders are supposed to also run with a center-of-mass energy of ~ 160 GeV, already tested at LEP. In analogy to Figure 9, in Figure 19 we show again cross section predictions for the process Zh in dependence of the mass of h , assuming a SM-like scalar. Note we here assume onshell production of Zh , which leads to a hard cutoff for $M_{h_1} \sim 70$ GeV. Detailed studies should in turn assume contributions from offshell Z s and h s as well.

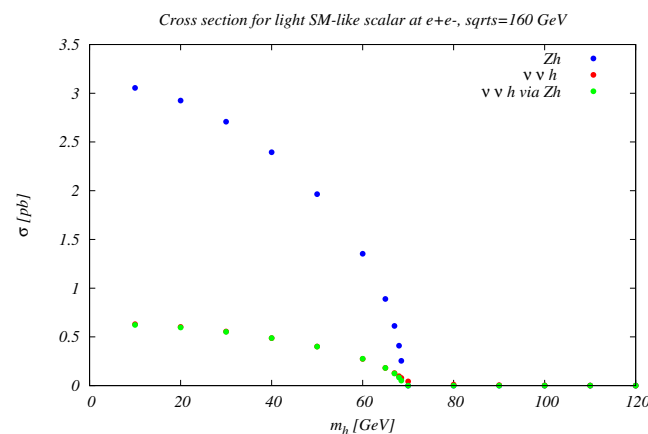


Figure 19. As Figure 9, for a com of 160 GeV. We assume onshell final states.

We see that for this lower com energy, there is basically no contribution to the $\nu_\ell \bar{\nu}_\ell h$ final state that does not originate from Zh . Using FCC-ee target luminosity for this energy, and again assuming a general suppression factor ~ 0.1 stemming from signal strength, we expect up to 10^6 events depending on the mass of the additional scalar.

For this center-of-mass energy, several searches exist which have already been performed at LEP and are summarized in [32,33], concentrating on $Z h$, $h_1 h_2$, and $h_1 h_1 h_1$ final states, which could be further pursued in future collider studies. We want to note that the luminosity at FCC-ee at this center of mass energy is exceeding LEP luminosity by several orders of magnitude.

Finally, we present a study that investigates various types of 2HDMs containing several neutral scalars [64], for a collider energy of 350 GeV. The authors perform a scan of the allowed parameter space and render predictions for the Higgs–Strahlung process as well as $\nu_\ell \bar{\nu}_\ell h$ final states with the scalar decaying into $b \bar{b}$ pairs. We show their results in Figure 20.

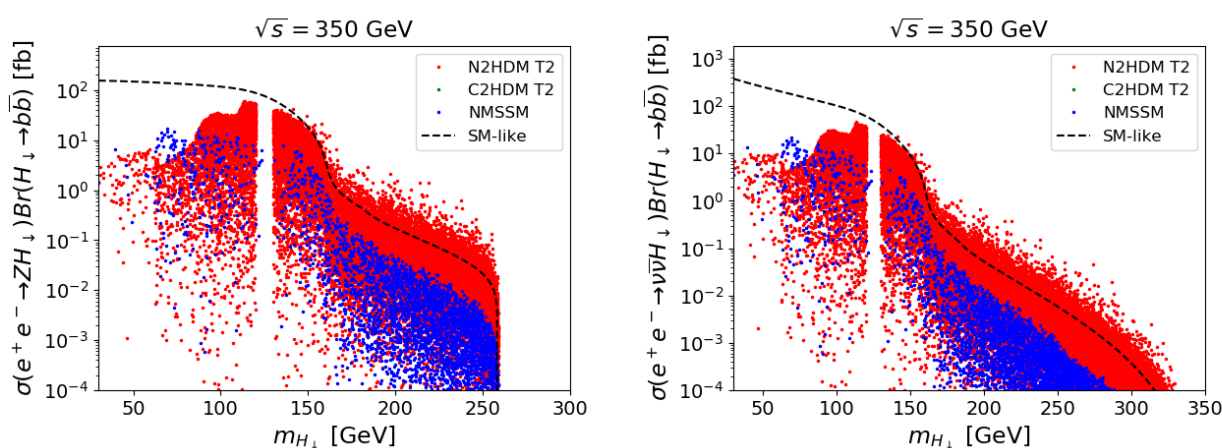


Figure 20. Achievable rates for various light scalar production modes at an e^+e^- collider with a center-of-mass energy of 350 GeV, in various 2HDM variant models. Figure taken from [64].

6. Conclusions

In this overview, I have presented several models and searches that investigate the sensitivity of future e^+e^- machines for scalars with masses $\lesssim 125$ GeV. This is based on several talks I have recently given and is thereby not meant to be inclusive. I have pointed to models that allow for such light scalars, as well as several references that either provide rates or pursue dedicated studies. I have also pointed to the connection of low-scalar searches at such colliders and the electroweak phase transition within certain models. My impression is that further detailed studies are called for, with a possible focus on so-called Higgs factories with center-of-mass energies around 240–250 GeV.

Funding: This research received no external funding.

Institutional Review Board Statement: Not applicable.

Informed Consent Statement: Not applicable.

Data Availability Statement: Data generated explicitly by the author for this review can be made available upon request.

Acknowledgments: I thank Sven Heinemeyer and the conveners of the CEPC workshop for inspiring me to set up an overview on these models. Several authors of the references cited here were also helpful in answering specific questions regarding their work.

Conflicts of Interest: The author declares no conflict of interest.

Note

- ¹ I thank V. Miralles for providing these plots.

References

- Available online: <https://twiki.cern.ch/twiki/bin/view/AtlasPublic/HiggsPublicResults> (accessed on 14 April 2022).
- Available online: <https://twiki.cern.ch/twiki/bin/view/CMSPublic/PhysicsResultsHIG> (accessed on 14 April 2022).
- Ellis, R.K.; European Strategy for Particle Physics Preparatory Group. Physics Briefing Book: Input for the European Strategy for Particle Physics Update 2020. *arXiv* **2019**, arXiv:1910.11775.
- European Strategy Group, 2020 Update of the European Strategy for Particle Physics. Technical Report, Geneva, 2020. Available online: <http://cds.cern.ch/record/2720129> (accessed on 14 April 2022).
- Robens, T. A short overview on low mass scalars at future lepton colliders-Snowmass White Paper. 2022 Snowmass Summer Study. *arXiv* **2022**, arXiv:2203.08210.
- Pruna, G.M.; Robens, T. Higgs singlet extension parameter space in the light of the LHC discovery. *Phys. Rev. D* **2013**, *88*, 115012. [\[CrossRef\]](#)
- Robens, T.; Stefaniak, T. Status of the Higgs Singlet Extension of the Standard Model after LHC Run 1. *Eur. Phys. J. C* **2015**, *75*, 104. [\[CrossRef\]](#)
- Robens, T.; Stefaniak, T. LHC Benchmark Scenarios for the Real Higgs Singlet Extension of the Standard Model. *Eur. Phys. J. C* **2016**, *76*, 268. [\[CrossRef\]](#)
- Ilnicka, A.; Robens, T.; Stefaniak, T. Constraining Extended Scalar Sectors at the LHC and beyond. *Mod. Phys. Lett. A* **2018**, *33*, 1830007. [\[CrossRef\]](#)
- Robens, T.; Stefaniak, T.; Wittbrodt, J. Two-real-scalar-singlet extension of the SM: LHC phenomenology and benchmark scenarios. *Eur. Phys. J. C* **2020**, *80*, 151. [\[CrossRef\]](#)
- Cepeda, M.; Gori, S.; Outschoorn, V.M.; Shelton, J. Exotic Higgs Decays. *arXiv* **2021**, arXiv:2111.12751.
- Robens, T. Constraining extended scalar sectors at current and future colliders. *arXiv* **2022**, arXiv:2203.17016.
- Carena, M.; Kozaczuk, J.; Liu, Z.; Ou, T.; Ramsey-Musolf, M.J.; Shelton, J.; Wang, Y.; Xie, K.P. Probing the Electroweak Phase Transition with Exotic Higgs Decays. 2022 Snowmass Summer Study. *arXiv* **2022**, arXiv:2203.08206.
- Coimbra, R.; Sampaio, M.O.P.; Santos, R. ScannerS: Constraining the phase diagram of a complex scalar singlet at the LHC. *Eur. Phys. J. C* **2013**, *73*, 2428. [\[CrossRef\]](#)
- Mühlleitner, M.; Sampaio, M.O.P.; Santos, R.; Wittbrodt, J. ScannerS: Parameter scans in extended scalar sectors. *Eur. Phys. J. C* **2022**, *82*, 198. [\[CrossRef\]](#)
- Bechtel, P.; Brein, O.; Heinemeyer, S.; Weiglein, G.; Williams, K.E. HiggsBounds: Confronting Arbitrary Higgs Sectors with Exclusion Bounds from LEP and the Tevatron. *Comput. Phys. Commun.* **2010**, *181*, 138–167. [\[CrossRef\]](#)
- Bechtel, P.; Brein, O.; Heinemeyer, S.; Weiglein, G.; Williams, K.E. HiggsBounds 2.0.0: Confronting Neutral and Charged Higgs Sector Predictions with Exclusion Bounds from LEP and the Tevatron. *Comput. Phys. Commun.* **2011**, *182*, 2605–2631. [\[CrossRef\]](#)
- Bechtel, P.; Brein, O.; Heinemeyer, S.; Stål, O.; Stefaniak, T.; Weiglein, G.; Williams, K.E. HiggsBounds-4: Improved Tests of Extended Higgs Sectors against Exclusion Bounds from LEP, the Tevatron and the LHC. *Eur. Phys. J. C* **2014**, *74*, 2693. [\[CrossRef\]](#)
- Bechtel, P.; Dercks, D.; Heinemeyer, S.; Klingl, T.; Stefaniak, T.; Weiglein, G.; Wittbrodt, J. HiggsBounds-5: Testing Higgs Sectors in the LHC 13 TeV Era. *Eur. Phys. J. C* **2020**, *80*, 1211. [\[CrossRef\]](#)
- Bechtel, P.; Heinemeyer, S.; Stål, O.; Stefaniak, T.; Weiglein, G. HiggsSignals: Confronting arbitrary Higgs sectors with measurements at the Tevatron and the LHC. *Eur. Phys. J. C* **2014**, *74*, 2711. [\[CrossRef\]](#)
- Bechtel, P.; Heinemeyer, S.; Klingl, T.; Stefaniak, T.; Weiglein, G.; Wittbrodt, J. HiggsSignals-2: Probing new physics with precision Higgs measurements in the LHC 13 TeV era. *Eur. Phys. J. C* **2021**, *81*, 145. [\[CrossRef\]](#)
- CMS Collaboration. First evidence for off-shell production of the Higgs boson and measurement of its width. *arXiv* **2022**, arXiv:2202.06923.
- Branco, G.C.; Ferreira, P.M.; Lavoura, L.; Rebelo, M.N.; Sher, M.; Silva, J.P. Theory and phenomenology of two-Higgs-doublet models. *Phys. Rept.* **2012**, *516*, 1–102. [\[CrossRef\]](#)
- Eberhardt, O.; Martínez, A.P.n.; Pich, A. Global fits in the Aligned Two-Higgs-Doublet model. *J. High Energy Phys.* **2021**, *5*, 005 [\[CrossRef\]](#)
- Pich, A.; Tuzon, P. Yukawa Alignment in the Two-Higgs-Doublet Model. *Phys. Rev. D* **2009**, *80*, 091702. [\[CrossRef\]](#)
- Pich, A. Flavour constraints on multi-Higgs-doublet models: Yukawa alignment. *Nucl. Phys. B Proc. Suppl.* **2010**, *209*, 182–187. [\[CrossRef\]](#)
- Combined Measurements of Higgs Boson Production and Decay Using Up to 139 fb⁻¹ of Proton-Proton Collision Data at $\sqrt{s} = 13$ TeV Collected with the ATLAS Experiment. Technical Report, CERN, Geneva, 2021. Available online: <https://atlas.web.cern.ch/Atlas/GROUPS/PHYSICS/CONFNOTES/ATLAS-CONF-2021-053> (accessed on 14 April 2022)
- Wang, L.; Yang, J.M.; Zhang, Y. Two-Higgs-doublet models in light of current experiments: A brief review. *arXiv* **2022**, arXiv:2203.07244.
- Abouabid, H.; Arhrib, A.; Azevedo, D.; Falaki, J.E.; Ferreira, P.M.; Mühlleitner, M.; Santos, R. Benchmarking Di-Higgs Production in Various Extended Higgs Sector Models. *arXiv* **2021**, arXiv:2112.12515.

30. Han, X.F.; Li, T.; Wang, H.X.; Wang, L.; Zhang, Y. Lepton-specific inert two-Higgs-doublet model confronted with the new results for muon and electron $g-2$ anomalies and multilepton searches at the LHC. *Phys. Rev. D* **2021**, *104*, 115001. [\[CrossRef\]](#)
31. Ferreira, P.M.; Gonçalves, B.L.; Joaquim, F.R. The hidden side of scalar-triplet models with spontaneous CP violation. *arXiv* **2021**, arXiv:2109.13179.
32. OPAL Collaboration; Abbiendi, G. Decay mode independent searches for new scalar bosons with the OPAL detector at LEP. *Eur. Phys. J. C* **2003**, *27*, 311–329. [\[CrossRef\]](#)
33. Schael, S.; Barate, R.; Brunelière, R.; De Bonis, I.; Decamp, D.; Goy, C.; Jézéquel, S.; Lees, J.P.; Martin, F.; Merle, E.; et al. Search for neutral MSSM Higgs bosons at LEP. *Eur. Phys. J. C* **2006**, *47*, 547–587. [\[CrossRef\]](#)
34. Abada, A.; Abbrescia, M.; AbdusSalam, S.S.; Abdyukhanov, I.; Abelleira Fernandez, J.; Abramov, A.; Aburaia, M.; Acar, A.O.; Adzic, P.R.; Agrawal, P.; et al. FCC-ee: The Lepton Collider: Future Circular Collider Conceptual Design Report Volume 2. *Eur. Phys. J. Spec. Top.* **2019**, *228*, 261–623. [\[CrossRef\]](#)
35. CEPC Study Group. CEPC Conceptual Design Report: Volume 2-Physics & Detector. *arXiv* **2018**, arXiv:1811.10545.
36. Cornell, A.S.; Deandrea, A.; Fuks, B.; Mason, L. Future lepton collider prospects for a ubiquitous composite pseudoscalar. *Phys. Rev. D* **2020**, *102*, 035030. [\[CrossRef\]](#)
37. Alwall, J.; Herquet, M.; Maltoni, F.; Mattelaer, O.; Stelzer, T. MadGraph 5: Going Beyond. *J. High Energy Phys.* **2011**, *06*, 128. [\[CrossRef\]](#)
38. Bambade, P.; Barklow, T.; Behnke, T.; Berggren, M.; Brau, J.; Burrows, P.; Denisov, D.; Faus-Golfe, A.; Foster, B.; Fujii, K.; et al. The International Linear Collider: A Global Project. *arXiv* **2019**, arXiv:1903.01629.
39. Drechsel, P.; Moortgat-Pick, G.; Weiglein, G. Prospects for direct searches for light Higgs bosons at the ILC with 250 GeV. *Eur. Phys. J. C* **2020**, *80*, 922. [\[CrossRef\]](#)
40. Barate, R. Search for the standard model Higgs boson at LEP. *Phys. Lett. B* **2003**, *565*, 61–75. [\[CrossRef\]](#)
41. Wang, Y.; Berggren, M.; List, J. ILD Benchmark: Search for Extra Scalars Produced in Association with a Z boson at $\sqrt{s} = 500$ GeV. *arXiv* **2020**, arXiv:2005.06265.
42. Liu, Z.; Wang, L.T.; Zhang, H. Exotic decays of the 125 GeV Higgs boson at future e^+e^- lepton colliders. *Chin. Phys. C* **2017**, *41*, 063102. [\[CrossRef\]](#)
43. Shelton, J.; Xu, D. Exotic Higgs Decays to Four Taos at Future Electron-Positron Colliders. 2022 Snowmass Summer Study. *arXiv* **2021**, arXiv:2110.13225.
44. Ma, S.; Wang, K.; Zhu, J. Higgs decay to light (pseudo)scalars in the semi-constrained NMSSM. *Chin. Phys. C* **2021**, *45*, 023113. [\[CrossRef\]](#)
45. Das, D.; Ellwanger, U.; Teixeira, A.M. LHC constraints on $M_{1/2}$ and m_0 in the semi-constrained NMSSM. *J. High Energy Phys.* **2013**, *4*, 117. [\[CrossRef\]](#)
46. Ellwanger, U.; Hugonie, C. The semi-constrained NMSSM satisfying bounds from the LHC, LUX and Planck. *J. High Energy Phys.* **2014**, *8*, 046. [\[CrossRef\]](#)
47. Nakamura, K.; Nomura, D. Charged Lepton Flavor Violation in the Semi-Constrained NMSSM with Right-Handed Neutrinos. *Phys. Lett. B* **2015**, *746*, 396–405. [\[CrossRef\]](#)
48. Wang, K.; Wang, F.; Zhu, J.; Jie, Q. The semi-constrained NMSSM in light of muon $g-2$, LHC, and dark matter constraints. *Chin. Phys. C* **2018**, *42*, 103109–103109. [\[CrossRef\]](#)
49. Kozaczuk, J.; Ramsey-Musolf, M.J.; Shelton, J. Exotic Higgs boson decays and the electroweak phase transition. *Phys. Rev. D* **2020**, *101*, 115035. [\[CrossRef\]](#)
50. Wang, Z.; Zhu, X.; Khoda, E.E.; Hsu, S.C.; Konstantinidis, N.; Li, K.; Li, S.; Ramsey-Musolf, M.J.; Wu, Y.; Zhang, Y.E. Study of Electroweak Phase Transition in Exotic Higgs Decays at the CEPC. 2022 Snowmass Summer Study. *arXiv* **2022**, arXiv:2203.10184.
51. Aaboud, M.; Aad, G.; Abbott, B.; Abeloos, B.; Abhayasinghe, D.K.; Abidi, S.H.; AbouZeid, O.S.; Abraham, N.L.; Abramowicz, H.; Abreu, H.; et al. Search for Higgs boson decays into a pair of light bosons in the $b\bar{b}\mu\mu$ final state in pp collision at $\sqrt{s} = 13$ TeV with the ATLAS detector. *Phys. Lett. B* **2019**, *790*, 1–21. [\[CrossRef\]](#)
52. Sirunyan, A.M.; Tumasyan, A.; Adam, W.; Ambrogio, F.; Asilar, E.; Bergauer, T.; Brandstetter, J.; Brondolin, E.; Dragicevic, M.; Erö, J.; et al. Search for an exotic decay of the Higgs boson to a pair of light pseudoscalars in the final state with two muons and two b quarks in pp collisions at 13 TeV. *Phys. Lett. B* **2019**, *795*, 398–423. [\[CrossRef\]](#)
53. Sirunyan, A.M.; Tumasyan, A.; Adam, W.; Ambrogio, F.; Asilar, E.; Bergauer, T.; Brandstetter, J.; Brondolin, E.; Dragicevic, M.; Erö, J.; et al. Search for an exotic decay of the Higgs boson to a pair of light pseudoscalars in the final state with two b quarks and two τ leptons in proton-proton collisions at $\sqrt{s} = 13$ TeV. *Phys. Lett. B* **2018**, *785*, 462. [\[CrossRef\]](#)
54. Aaboud, M.; Aad, G.; Abbott, B.; Abeloos, B.; Abhayasinghe, D.K.; Abidi, S.H.; AbouZeid, O.S.; Abraham, N.L.; Abramowicz, H.; Abreu, H.; et al. Search for the Higgs boson produced in association with a vector boson and decaying into two spin-zero particles in the $H \rightarrow aa \rightarrow 4b$ channel in pp collisions at $\sqrt{s} = 13$ TeV with the ATLAS detector. *J. High Energy Phys.* **2018**, *10*, 031. [\[CrossRef\]](#)
55. Sirunyan, A.M.; Tumasyan, A.; Adam, W.; Ambrogio, F.; Asilar, E.; Bergauer, T.; Brandstetter, J.; Dragicevic, M.; Erö, J.; Del Valle, A.E.; et al. Search for light pseudoscalar boson pairs produced from decays of the 125 GeV Higgs boson in final states with two muons and two nearby tracks in pp collisions at $\sqrt{s} = 13$ TeV. *Phys. Lett. B* **2020**, *800*, 135087. [\[CrossRef\]](#)

-
56. Aad, G.; Abbott, B.; Abdallah, J.; Aben, R.; Abolins, M.; AbouZeid, O.S.; Abramowicz, H.; Abreu, H.; Abreu, R.; Abulaiti, Y.; et al. Search for Higgs bosons decaying to aa in the $\mu\mu\tau\tau$ final state in pp collisions at $\sqrt{s} = 8$ TeV with the ATLAS experiment. *Phys. Rev. D* **2015**, *92*, 052002. [[CrossRef](#)]
 57. Carena, M.; Liu, Z.; Wang, Y. Electroweak phase transition with spontaneous Z_2 -breaking. *J. High Energy Phys.* **2020**, *8*, 107. [[CrossRef](#)]
 58. Chun, E.J.; Mondal, T. Searching for a Light Higgs Boson via the Yukawa Process at Lepton Colliders. *Phys. Lett. B* **2020**, *802*, 135190. [[CrossRef](#)]
 59. Abi, B.; Albahri, T.; Al-Kilani, S.; Allspach, D.; Alonzi, L.P.; Anastasi, A.; Anisenkov, A.; Azfar, F.; Badgley, K.; Baeßler, S.; et al. Measurement of the Positive Muon Anomalous Magnetic Moment to 0.46 ppm. *Phys. Rev. Lett.* **2021**, *126*, 141801. [[CrossRef](#)]
 60. Akeroyd, A.G.; Moretti, S.; Song, M. Light charged Higgs boson with dominant decay to a charm quark and a bottom quark and its search at LEP2 and future e^+e^- colliders. *Phys. Rev. D* **2020**, *101*, 035021. [[CrossRef](#)]
 61. Sirunyan, A.M.; Tumasyan, A.; Adam, W.; Ambroggi, F.; Asilar, E.; Bergauer, T.; Brandstetter, J.; Brondolin, E.; Dragicevic, M.; Erö, J.; et al. Search for a standard model-like Higgs boson in the mass range between 70 and 110 GeV in the diphoton final state in proton-proton collisions at $\sqrt{s} = 8$ and 13 TeV. *Phys. Lett. B* **2019**, *793*, 320–347. [[CrossRef](#)]
 62. Heinemeyer, S.; Li, C.; Lika, F.; Moortgat-Pick, G.; Paasch, S. A 96 GeV Higgs Boson in the 2HDM plus Singlet. *arXiv* **2021**, arXiv:2112.11958.
 63. Biekötter, T.; Heinemeyer, S.; Weiglein, G. Mounting evidence for a 95 GeV Higgs boson. *arXiv* **2022**, arXiv:2203.13180.
 64. Azevedo, D.; Ferreira, P.; Mühlleitner, M.M.; Santos, R.; Wittbrodt, J. Models with extended Higgs sectors at future e^+e^- colliders. *Phys. Rev. D* **2019**, *99*, 055013. [[CrossRef](#)]